Engineering Applications of Artificial Intelligence 161 (2025) 112252

Contents lists available at ScienceDirect

Engineering Applications of Artificial Intelligence

journal homepage: www.elsevier.com/locate/engappai

Advanced machine learning techniques for predicting wear performance in graphene oxide particulate interpenetrating polymer network composites

Eastus Russel [a], S. Madhu [b,*], Judy S [b], Edwin Geo Varuvel [c,d,**], G.B. Santhi [e], G. Suresh [f], Femilda Josephin J.S[g], Mohammed F. Albeshr [h], Farzad Kiani [i]

[a] Department of Mechanical Engineering, Sri Muthukumaran Institute of Technology, Chennai, India
[b] Saveetha School of Engineering, Saveetha Institute of Medical and Technical Sciences, Saveetha University, Chennai, India
[c] Department of Mechanical Engineering, Faculty of Engineering and Natural Sciences, Istinye University, Istanbul, Turkiye
[d] Mechanical Science Institute, Vilnius Gediminas Technical University, Plytinės Str. 25, 10105, Vilnius, Lithuania
[e] Department of Computer Science and Engineering, New Prince Shri Bhavani College of Engineering and Technology, Chennai, India
[f] Department of Mechanical Engineering, Rajalakshmi Institute of Technology, Chennai, India
[g] Department of Computer Engineering, Faculty of Engineering and Natural Sciences, Istinye University, Istanbul, Turkiye
[h] Department of Chemistry, College of Sciences, King Saud University, P.O. Box. 2455, Riyadh, 11451, Saudi Arabia
[i] Data Science Application and Research Center (VEBIM), Fatih Sultan Mehmet Vakif University, Istanbul, Turkiye

ARTICLE INFO

Keywords:
Graphene oxide
Wear rate
Coefficient of friction
Linear regression
Decision tree
Random Forest Algorithm

ABSTRACT

This research investigates the wear behavior of hybrid polymeric composites made from synthetic glass and natural cotton fibers, reinforced with varying proportions of Graphene Oxide (GO) (0 %, 1 %, 3 %, 5 %, 7 %, 9 %). The effect of fiber arrangement and Graphene Oxide (GO) incorporation on wear rate and Coefficient of Friction (CoF) was evaluated using the Pin-On-Disk method, with analysis based on Taguchi's L_{32} Orthogonal Array. The optimal parameters were found at 6 min, 5 % GO, 300 *revolutions* per *minute* (rpm) speed, 20 mm (mm) track diameter, and 10 N (N) load, achieving a minimum wear rate of 0.612×10^{-4} cubic millimeters per newton-meter (mm^3/N-m) and a CoF of 0.151. Predictive modeling was performed to predict the wear rate and coefficient of friction using supervised machine learning algorithms, including Linear Regression, Decision Tree, and Random Forest, to forecast material behavior. Performance evaluation using Confusion Matrix, Distribution Analysis, and various metrics showed that the Decision Tree model excelled, achieving near-perfect predictive power with a Mean Squared Error (MSE) of 0 and an R-squared value of 0.9999. The model demonstrated 100 % accuracy, with precision, recall, and F1-scores all equal to 1. This research demonstrates the effectiveness of combining natural and synthetic fibers with GO, along with the predictive power of machine learning in optimizing material properties.

Acronyms

IPN	Interpenetrating Polymer Network	GA	Genetic Algorithm
GO	Graphene Oxide	SEM	Scanning Electron Microscopy
AI	Artificial Intelligence	RF	Random Forest
ANN	Artificial neural network	DT	Decision Tree
GFRP	Glass Fiber-reinforced Plastics	LR	Linear Regression
GSM	Gram per Square Meter	MSE	Mean Squared Error
MAE	Mean Absolute Error	CSV	Comma -Separated Values

(*continued on next column*)

(*continued*)

R^2	R-squared	CoF	Coefficient of Friction
UHMWPE	Ultra-High Molecular Weight Polyethylene	PMMA	Polymethyl Methacrylate
PEEK	Polyether Ether Ketone	FIS	Fuzzy Inference Systems
Rp3	Rocket Projectile 3 inch	DMD	D-optimal Mixture Design
ANFIS	Adaptive Neuro-Fuzzy Inference System	ML	Machine Learning
RSM	Response Surface Methodology	S/N	Signal-to-Noise
PTFE	PolyTetraFluoroEthylene	AD	Alzheimer's Disease

(*continued on next page*)

* Corresponding author.
** Corresponding author. Department of Mechanical Engineering, Faculty of Engineering and Natural Sciences, Istinye University, Istanbul, Turkiye.
E-mail addresses: mathumarine@gmail.com (S. Madhu), vedwingeo@gmail.com (E.G. Varuvel).

https://doi.org/10.1016/j.engappai.2025.112252
Received 29 January 2025; Received in revised form 23 July 2025; Accepted 5 September 2025
Available online 17 September 2025

(*continued*)

mm	Millimetre	mm3	Cubic Millimetre
rpm	Revolutions per Minute	mm^3/N-m	Cubic Millimetre/ Newton-metre
N	Newton	k-NN	k – Nearest Neighbour
Mins	Minutes	wt.%	Weight Percentage

1. Introduction

In recent decades, escalating industrial demands for material technology have prompted the need for new materials characterized by high durability. The significance of wear analysis, which indicates material strength, has predominantly grown to a massive level. Adhesive wear in polymer composites is considered a complex process, influenced by operational conditions and the properties of the composite materials (Yi Hsu et al., 2023). Key wear indicators, such as surface roughness, wear rate, and friction coefficient, are crucial in assessing material wear. Additionally, the consequences of wear include surface roughness, component weakening, surface degradation, and a shortened functional lifecycle of components (Mohammed et al., 2023). Given that such effects can lead to failures in manufacturing applications, the importance of polymer-based composites and their wear resistance properties has become more essential (Dayalan et al., 2023). Glass Fiber Reinforced (GFRP) composite materials find extensive use across various applications due to their remarkable attributes, including high specific strength, exceptional chemical resistance, lightweight nature, superior elasticity, excellent corrosion resistance, and impressive thermal stability (Zaghloul et al., 2023). Additionally, GFRP composites can incorporate additives and fillers, such as thermoplastic tensile additives like polyvinyl acetate, polystyrene, and plasticizers (Sharma et al., 2018). Graphene and its derivatives, particularly Graphene Oxide (GO), are widely recognized for enhancing polymer composites' mechanical, thermal, and tribological properties. Recent research highlights their effectiveness in improving wear resistance and reducing friction. The author reported that incorporating 0.10–0.25 wt% reduced GO into UHMWPE (Ultra-High Molecular Weight Polyethylene) composites led to a significant 48 % reduction in the coefficient of friction, along with increased hardness and modulus (Soares et al., 2022). It is demonstrated that PMMA (Polymethyl Methacrylate) coatings reinforced with 5 wt% Graphene nanoplatelets exhibited optimal wear performance, although excess filler content adversely affected stability (Salasel et al., 2023). It is found that GO improved the interfacial bonding between aramid fibers and epoxy, enhancing both tribological and mechanical properties (Feng et al., 2024). Additionally, the authors conducted a detailed Taguchi-based analysis on GO-reinforced PEEK (Polyether Ether Ketone) composites and identified that the optimal filler content and test conditions significantly minimized both wear rate and coefficient of friction, emphasizing GO's role in improving load-bearing capacity and wear resistance in engineering thermoplastics (Sharma and Mishra, 2024).

Within the existing and available recent literature, numerous studies delve into the application of artificial intelligence methods for estimating various types of material wear properties. As well, mathematical models that predict wear rates by assessing material loss under solid particle impact conditions enable the replication of multiple experimental tests. Nevertheless, forecasting wear values for composite materials proves intricate, involving complex and nonlinear phenomena. Artificial intelligence methods, including expert systems such as Artificial Neural Network (ANN) and Fuzzy Inference Systems (FIS), exhibit advantageous properties for modelling nonlinear systems. ANN, in particular, could establish a multivariable and continuous approximation of nonlinear processes, mapping relationships between input and output variables. They are also adept at discrete function approximation, termed "classification," which extracts the operating conditions of a machine. To address this, a three-layered ANN structure is proposed for predicting the erosion wear characteristics of a material. The inputs and outputs for this model include erodent discharge rate, iron mud content, impingement angle, erodent velocity, and erosion rate, respectively (Sonawane et al., 2022).

ANNs are employed for predicting wear on C120 and Rp3 steel surfaces reinforced with short glass fibers, particularly under linear contact conditions. The inclusion of these composite mixtures introduces nonlinearity into machining processes, posing challenges for wear predictions using analytical models across varying pressures and speeds. Likewise, an ANN prediction model is utilized for optimizing the wear rate of composites like epoxy combined with E-glass fiber and carbon particles. This approach aids in minimizing performance metrics such as friction coefficient and weight loss. Artificial neural networks are applied to predict wear on surfaces of C120 and Rp3 steel reinforced with short glass fibers, specifically under conditions of linear contact. The incorporation of these composite mixtures introduces nonlinearity into machining processes, presenting challenges for wear predictions using analytical models across varying pressures and speeds (Friemann Dashtbozorg et al., 2023).

Additionally, an ANN prediction model is employed to optimize the wear rate of composites, such as those consisting of epoxy combined with E-glass fiber and carbon particles. This modelling approach contributes to the reduction of performance metrics, including weight loss and friction coefficient. The utilization of Genetic Algorithm (GA) and multiple linear regression analysis (Taguchi Method) for tuning parameters of Artificial Neural Networks (ANN) has been proven as a successful tool utilizing enhancing the wear rate of composites. In an equivalent investigation focusing on ANNs, the computational simulation and prediction of erosive wear response in glass fiber composites filled with particulates considered variables such as impact angle, impact velocity, temperature, and erodent size. Furthermore, the investigators extensively analyzed the effects of impact speed and impact angle in a distinct study (Abed et al., 2023).

Taguchi's orthogonal array approach has been employed to determine optimal parameter settings for minimizing wear rates. In a discrete study, Padhi and Satapathy meticulously examine the morphology of worn surfaces, including the fracture of short glass fibers, wear tracks, and plastic deformation levels through Scanning Electron Microscopy (SEM) analysis. Researchers validate the significant capability of a well-trained Artificial Neural Network through various experimental results. In line with the above, another methodology has been proposed which combines the planning of experiments with the D-optimal Mixture Design (DMD) method and effective optimization using analysis methods such as ANN and Genetic Algorithms (GA). This approach meaningfully aims to assist decision-making experts in determining the optimal ratio of ingredients in the mixture of polytetrafluoroethylene reinforced polycarbonate short glass fiber composites (Elenchezhian et al., 2021).

In this present investigation, specimens that have been fabricated from cotton and glass fiber-reinforced composites undergo wear testing. The primary objective is to identify the optimal material composition and operational parameters for enhanced wear resistance. The prevailing literature survey typically compares Artificial Neural Network (ANN) estimation models with experimental results, wherein ANN commonly consider factors such as load, speed, and the percentage of

Table 1
Composite materials and machine learning models.

References	Study Focus	Machine Learning Model Used
Mohana Krishnudu et al., 2023	Adaptive Neuro-Fuzzy Inference System (ANFIS) applied to predict abrasive wear behavior in abutilon indicium fiber-reinforced epoxy composites.	ANFIS
Althaf Hasan Khan et al., 2022	Regression-based models were used to forecast the wear behavior of aluminum alloy composites with $ZrSiO_4$.	Regression-based Models
Formisano et al. (2021)	Neural network prediction models are used for estimating the wear behavior of SiC micro particle-filled epoxy resins.	Neural Networks
Faisal and Mohammed (2020)	Machine learning techniques were applied to predict the hardness and wear behavior of friction-stir-processed cast A319 aluminum alloys.	Machine Learning Techniques
Bright et al. (2022)	Response Surface Methodology (RSM) was used to predict dry sliding wear behavior in AA6082 matrix composites.	Response Surface Methodology (RSM)
Justin Abraham Baby et al. (2025)	Al6061/WC composites with tungsten carbide show enhanced wear resistance, ideal for industrial use.	Not Specified
Haja Syeddu Masooth et al., 2022	AA6061 nanocomposites with graphene and zirconia offer enhanced wear resistance, predicted by ANN and fuzzy models.	Artificial Neural Network (ANN) and Sugeno-type Fuzzy Inference Systems
Ragupathy et al. (2021)	ANFIS and RSM applied to predict dry sliding wear response of AlMg1SiCu/Silicon Carbide/Molybdenum Disulfide hybrid composites.	ANFIS and RSM
Sosimi et al. (2020)	Artificial Neural Networks (ANN) are used to analyze wear behavior in Al-$CaCO_3$ composites.	ANN
Yilmaz et al. (2021)	The ANFIS model was used to estimate adhesive wear behavior in glass fiber-reinforced polyester composites.	ANFIS
Alhaji Ibrahim et al., 2022	Hybrid support vector regression models were applied to optimize and predict tribological behavior in PTFE composites.	Hybrid Support Vector Regression
D. et al. (2022)	ANN models were applied to investigate tribological behavior in Aluminium-WC metal matrix composites.	ANN

additive in the composite (%). This study introduces an Adaptive Neuro-Fuzzy Inference System (ANFIS) sub-clustering-based prediction model for estimating the wear behavior of glass fiber-reinforced polyester composites across varying material concentrations, loads, and speeds. The model effectively extracts optimal concentrations and operational parameters, aiming to minimize the wear rate (Valishin et al., 2023). Table 1 provides the literature review on composite materials and the Machine Learning Models used. The novelty of this research lies in the integration of Graphene Oxide (GO) into Interpenetrating Polymer Network (IPN) composites reinforced with both synthetic glass and natural cotton fibers, and the application of advanced Machine Learning (ML) algorithms to accurately predict wear performance.

The integration of composite-nanoparticle-enriched lubricant oils represents a significant advancement in frictional performance enhancement, as demonstrated through machine learning optimization. This approach allows for precise tuning of nanoparticle content to improve wear resistance and energy efficiency in lubricants, showcasing machine learning's potential in material engineering (Reddy et al., 2024). Screening preclinical Alzheimer's Disease (AD) cohorts through a composite machine learning model highlights the versatility of machine learning in healthcare. By utilizing remote cognitive testing, this model provides an efficient and accurate framework for early AD detection, crucial for timely intervention (Liu et al., 2023). Predicting maximum tensile stress in plain-weave composite laminates with interacting holes has been achieved through stacked machine learning algorithms. These models deliver robust stress predictions, essential for applications in composite structures requiring high accuracy and durability (Bagherzadeh et al., 2023). Machine learning-aided design has become pivotal in developing reinforced polymer composites and hybrid material systems. This approach streamlines the design process, allowing for quicker optimization and enhanced material performance, which is critical in advancing composite applications (Okafor et al., 2023). Hybrid additive manufacturing processes benefit greatly from machine learning optimization, as seen in the production of sustainable polylactic acid-carbon fiber composite structures. Machine learning fine-tunes manufacturing parameters, contributing to eco-friendly production and superior material quality (Thakur et al., 2023). Fracture energy assessment in strain-hardening fiber-reinforced cementitious composites has been improved through machine learning techniques. This approach provides accurate predictions that enhance the performance and resilience of cementitious materials, addressing essential needs in engineering (Raja et al., 2024).

Existing literature may lack comprehensive studies on the wear behavior specific to graphene oxide-reinforced IPN composites, especially under varying operational conditions. Although machine learning has been applied in wear prediction, its application in the specific context of graphene oxide IPN composites remains limited. This study explores the wear behavior of hybrid polymeric composites made from synthetic glass and natural cotton fibers, reinforced with varying proportions of Graphene Oxide (GO). The sequence of fibers and GO incorporation was evaluated for their influence on wear rate and Coefficient of Friction (CoF), using the Pin-On-Disk method and Taguchi's L_{32} Orthogonal Array. Predictive modelling was performed using supervised machine learning algorithms.

2. Materials and methods

2.1. Materials

In the fabrication of the Interpenetrating Polymer Network (IPN) composite, strengthened with cotton fibers and infused with graphene oxide particles, the hand lay-up technique was utilized. Furthermore, various ratios of particulates were incorporated to enhance the overall physical characteristics of the IPN composite (Russel et al., 2023a). The experimental raw materials used in this study include cotton fiber, E-glass fiber, graphene oxide, epoxy resin, and vinyl ester resin. Cotton fiber, sourced locally from the Tamil Nadu region of India near Chennai, is a natural single-cell fiber known for its softness, durability, and moisture absorption up to 2.7 times its weight. The fibers underwent cleaning using a motorized automatic combing mechanism to remove impurities and were then treated to prepare them for composite fabrication. E-glass fiber, procured from Sakthi Fibres, Chennai, was in the form of 350 GSM biaxially woven mats and serves as a reinforcing material due to its high strength. Graphene oxide of a thickness of 10 μm was used in this research.

GO consists of oxygen-containing functional groups like epoxy, hydroxyl, carboxyl, and carbonyl, and was used as a nano-filler to enhance the mechanical performance of the composite. Epoxy resin, a thermosetting polymer formed by the reaction of bisphenol A with epichlorohydrin, offers excellent chemical resistance, minimal shrinkage, and high cross-linking ability upon curing with a hardener. Vinyl ester, a hybrid resin with structural features between polyester and epoxy, has high durability, strong mechanical properties, and good water resistance due to its long double bonds and Oxygen Hydrogen groups that facilitate adhesion to fiber surfaces. The volume percentage of Graphene Oxide (GO) in the composite plays a crucial role in determining its mechanical and physical properties. GO is dispersed uniformly into the epoxy-vinyl ester resin blend. This dispersion is achieved through techniques such as sonication and mechanical stirring, which help break down agglomerates and ensure even distribution of the GO sheets within the matrix. As the GO content increases from 0 % to 9 %, the proportion of E-glass fiber and cotton fiber decreases from 60 % to 51 %. In comparison, the IPN matrix (epoxy + vinyl ester) remains constant at 40 %. Glass fibers add high tensile strength and durability, while cotton fibers contribute flexibility and environmental sustainability. GO enhances the mechanical and wear resistance properties of the composite by improving interfacial bonding within the matrix. A 50:50 blend of epoxy (LY556) and vinyl ester (SKR4101) resins forms the matrix, combining epoxy's strength and stress distribution with vinyl ester's chemical resistance and toughness. Together, these materials create a composite with optimized strength, wear resistance, and eco-friendly attributes.

2.2. Fabrication of interpenetrating polymer network composite laminate

The hybrid IPN laminate was crafted using a manual lay-up approach. Initially, a 350 GSM piece of E-glass simple woven fabric was cut to the specified size and pre-dried for approximately 1 h at 140 °C to eliminate absorbed moisture. Similarly, the required amount of cotton fabric was also pre-dried and cut for fabrication purposes. A suitable amount of Polyvinyl alcohol, serving as a drying agent, was applied as a gel coat to pre-treat the mold's surface. The necessary percentage of IPN was then applied with a brush onto the mold. Subsequently, an E-Glass fiber layer (160 × 160 mm) was laid on top of the resin, and the excess resin was blended out using rolling wheels. Following this, the next layer of cotton fiber was positioned over the wetted E-Glass fiber. Similarly, one layer of glass and another layer of cotton fibers were added simultaneously to create a 5-ply laminate. Care was taken to maintain the fabric in a straight line throughout the process. The lamination was allowed to air-dry at room temperature for approximately 24 h. The specimens for testing were cut from the produced laminates, with dimensions of 32 x 8 × 3.2 mm. Fig. 1 shows the methodology of the fabricated interpenetrating polymer network (IPN) composites (Russel et al., 2023b).

SEM analysis revealed typical fracture mechanisms such as fiber pullout, matrix cracking, voids, and fiber scissoring, regardless of particulate content shown in Fig. 2. At 1 % GO, good interfacial adhesion was observed, with signs of stress transfer from matrix to fiber, scissored fibers, and shear cup formations indicating improved energy absorption compared to the neat IPN matrix. With 3 % and 5 % GO, further improvement in interfacial bonding and uniform particulate dispersion contributed to maximum stress absorption. However, at 7 % and 9 % GO, agglomeration, voids, and matrix-rich regions disrupted uniform bonding, reducing stress transfer efficiency and causing early delamination. Thus, up to 5 % GO is optimal for enhancing fiber-matrix adhesion and mechanical performance.

3. Wear test details

The wear test was conducted using a pin-on-disc wear test rig according to ASTM G99 standards. The specimens for testing were cut from the produced laminates, with dimensions of 32 x 8 × 3.2 mm^3. In

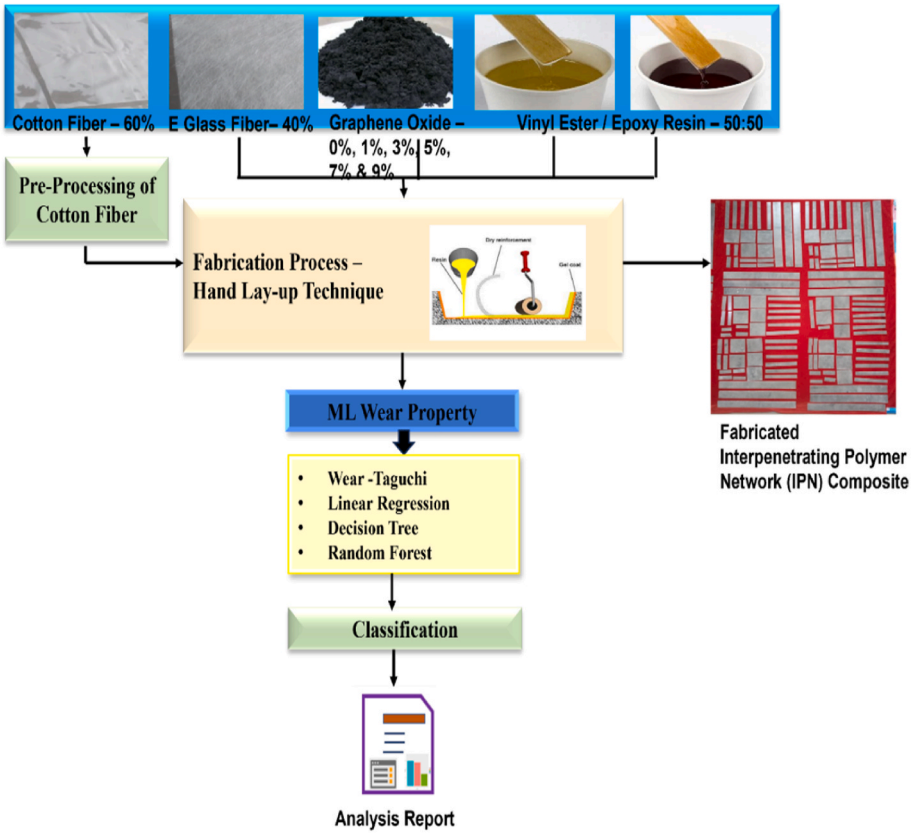

Fig. 1. Fabrication and wear prediction methodology of IPN composite.

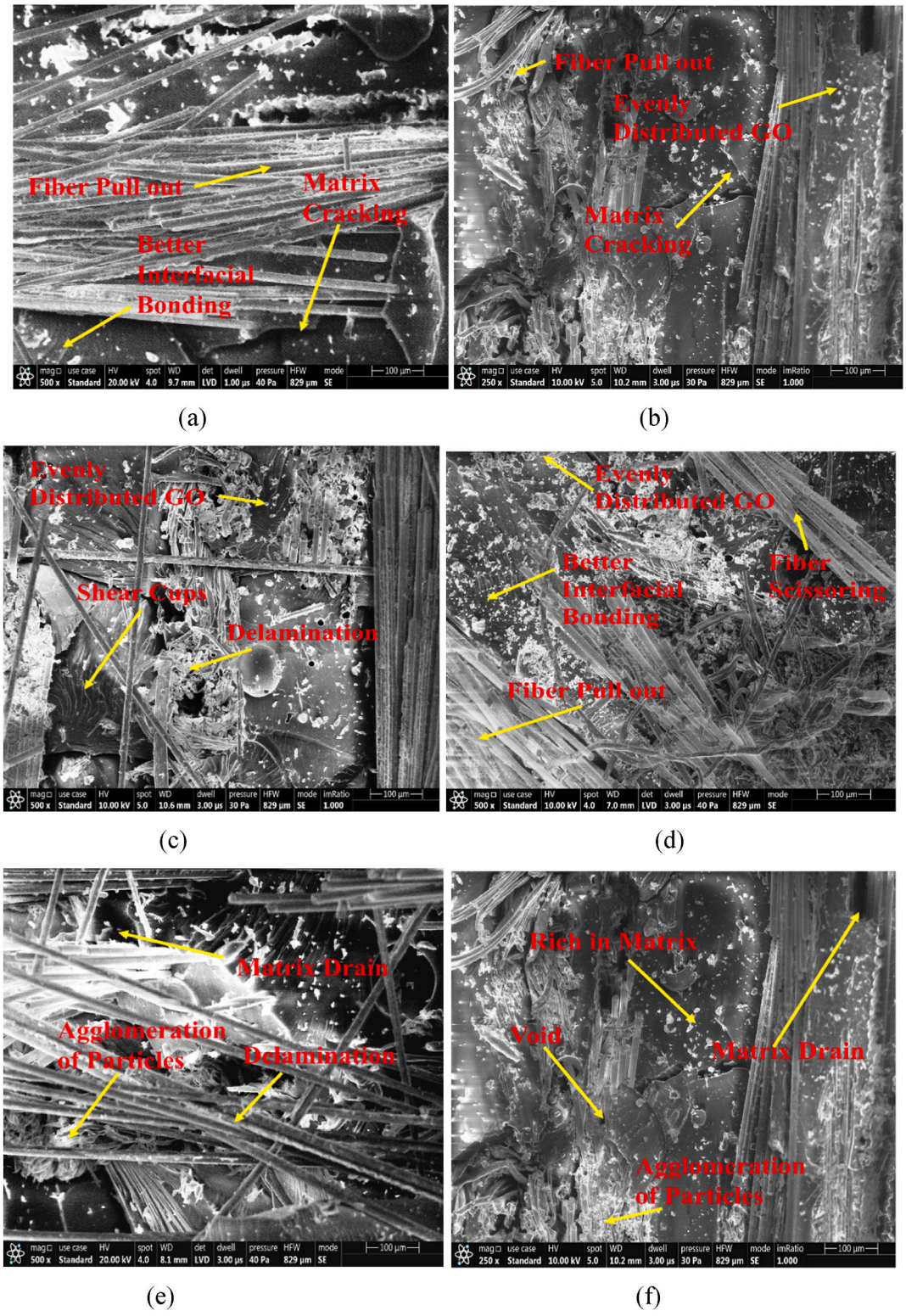

Fig. 2. SEM images of the fractured cotton/E-glass fiber reinforced vinyl ester/epoxy resin (Graphene Oxide loaded) hybrid IPN composites at (a) 0 wt% GO, (b) 1 wt % GO, (c) 3 wt% GO, (d) 5 wt% GO, (e) 7 wt% GO and (f) 9 wt% GO.

this setup, a pin with a radius tip is positioned perpendicular to a flat circular disk. The pin specimen, often a tightly held ball, remains stationary while the disk specimen rotates around its centre, creating a circular sliding path on the disk's surface. The disk plane can be oriented vertically or horizontally. Typically, an arm or lever with attached weights applies a set load to press the pin against the disk, though pneumatic or hydraulic loading methods can also be used. Wear is assessed by measuring either the linear dimensions or the weight of both specimens before and after testing. Tests were performed under varying loads of 10 N, 15 N, 20 N, and 25 N across a sliding distance of 380 m. After measuring the specimens at different sliding distances, weight loss was calculated to determine wear, defined as the reduction in specimen

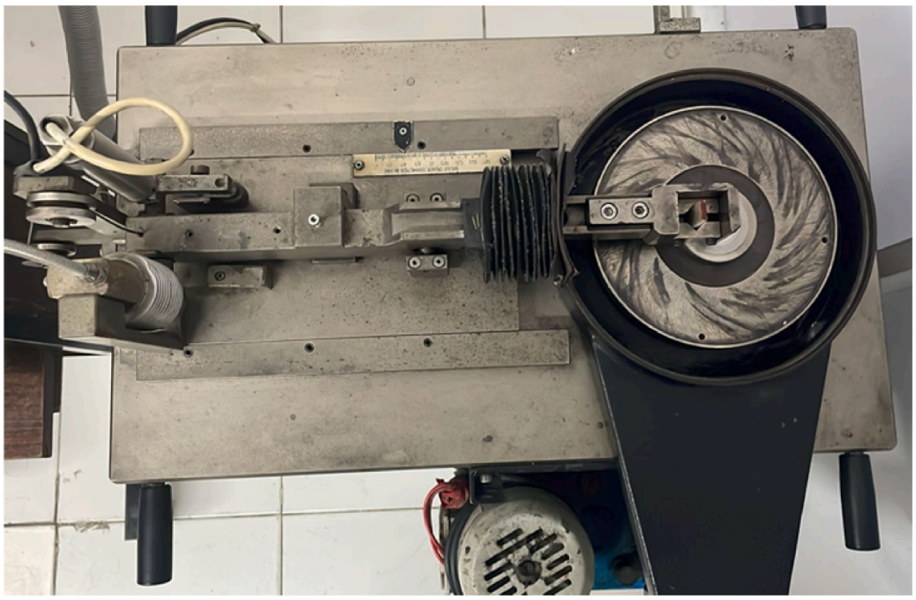

Fig. 3. Wear testing equipment.

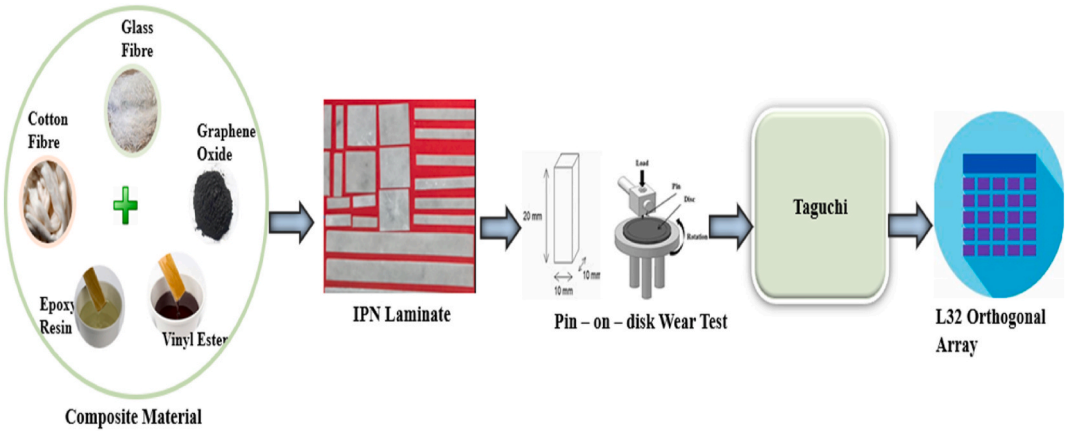

Fig. 4. Schematic illustration of the wear process of the fabricated IPN composite.

weight. Each test used a new specimen, and the shaft surface was cleaned of debris after each trial before beginning a new test. Wear was measured before and after each experiment using precision balance scales with an accuracy of 10^{-4} g. Fig. 3 shows the wear-testing machine used for this investigation.

Fig. 4 shows the illustration of the wear process of the fabricated IPN composite. The illustrative representation provides a visual overview of the conclusive outcome derived from Taguchi, which takes the form of the L_{32} Orthogonal Array.

The five control variables in this tribological experiment were load, sliding time, speed, track diameter, and graphene oxide reinforcement fraction, all of which were varied to varying degrees. The influence of parameters on the desired output has been ascertained through the use of Taguchi-based orthogonal arrays, which can evaluate two or even more parameters independently and simultaneously that will impact the variability of a particular process characterisation with the least amount of tests. It was determined that the L_{32} orthogonal cluster was appropriate in light of these control variables. Furthermore, no consideration is given to noise issues in this study. Table 2 states the level and control factors. This particular array is strategically organized to serve as the foundational dataset for the proposed methodology.

Table 2
Control factors and levels.

Control Factors	Unit	Levels			
		1	2	3	4
Time (A)	minutes	6	12		
% of GO (B)		1	3	5	7
Speed (C)	rpm	300	400	500	600
Diameter of Track (D)	mm	20	24	28	32
Load (E)	N	10	15	20	25

The control factors and levels were carefully selected based on both practical relevance and literature support. Time (6 and 12 min) was chosen to compare short-term and extended wear behaviours without redundancy, as wear trends typically stabilize early. The percentage of GO (1, 3, 5, 7 %) spans a meaningful range: lower levels have minimal effect, 3–5 % is generally optimal, and levels beyond 5 % risk agglomeration, which can reduce performance. Speed levels (300–600 rpm) simulate realistic sliding conditions, with 100 rpm increments capturing kinetic effects without causing thermal degradation. Track diameter (20–32 mm) affects sliding distance and tangential velocity; the selected

levels offer realistic variation while maintaining consistent contact mechanics. Load values (10–25 N) represent increasing operational stress, allowing clear observation of pressure effects on wear and friction under light to moderate service conditions.

3.1. Method

The research methodology begins with the utilization of the Taguchi method, employing an L_{32} Orthogonal array, to generate a dataset. Working with a dataset of only 32 entries poses challenges in machine learning, primarily due to the risk of overfitting, where the model may perform well on the training data but fail to adapt to new, unseen data. In this scenario, complex algorithms like deep learning models and neural networks are not suitable, as they need large datasets for effective training. Instead, simpler models like Decision Trees, Linear Regression, or k-NN (k-Nearest Neighbour) are more appropriate as they are less dependent on large datasets. The schematic outlines the sequential steps involved in the prediction process, emphasizing the key stages and interactions of these algorithms within the framework.

The dataset comprising 32 experimental samples generated using the Taguchi L32 Orthogonal Array is split into 80 % training data (26 samples) and 20 % testing data (6 samples) to evaluate model generalization on unseen instances. The dataset includes input features such as Graphene Oxide (wt.%), Time (min), Speed (rpm), Load (N), and Track Diameter (mm), with target outputs being Wear and Coefficient of Friction (CoF). The algorithm starts by loading the dataset, extracting features and targets, and then performing the train-test split. Machine learning models such as Linear Regression, Decision Tree, and Random Forest are each trained using the training data and tested on separate testing data. Linear Regression fits a linear equation, Decision Tree uses rule-based partitioning, and Random Forest leverages an ensemble of decision trees to enhance prediction accuracy. The resulting predictions from all models are compared to assess their effectiveness in estimating Wear and CoF values. Fig. 5 provides a detailed representation of the proposed methodology devised for predicting wear and the coefficient of friction. This methodology is centered around the application of machine learning algorithms, namely Linear Regression, Decision Tree, and Random Forest.

Algorithm 1 delineates the step-by-step procedure for predicting Wear and Coefficient of Friction by employing various Machine Learning Models. The algorithm encompasses the key stages involved in processing the input data, training the models, making predictions, and assessing the performance of each model in terms of Wear and Coefficient of Friction. The details provided in the algorithm offer a comprehensive understanding of how the predictive analysis is executed using machine learning techniques. Table 3 shows the dataset, L_{32} Orthogonal Array with features and target variables.

Table 3
Dataset with features and target variables.

SNo	Time (Mins)	% of GO	Speed (rpm)	Diameter of Track (mm)	Load (N)	Wear ($x10^{-4}$ mm^3/N-m)	CoF (μ)
1	6	1	300	20	10	1.100	0.243
2	6	1	400	24	15	1.321	0.252
3	6	1	500	28	20	1.580	0.261
4	6	1	600	32	25	1.820	0.272
5	6	3	300	20	10	0.812	0.209
6	6	3	400	24	15	0.901	0.219
7	6	3	500	28	20	1.037	0.232
8	6	3	600	32	25	1.110	0.241
9	6	5	300	20	10	0.612	0.151
10	6	5	400	24	15	0.701	0.163
11	6	5	500	28	20	0.813	0.172
12	6	5	600	32	25	0.911	0.181
13	6	7	300	20	10	2.649	0.251
14	6	7	400	24	15	2.744	0.263
15	6	7	500	28	20	2.861	0.272
16	6	7	600	32	25	2.950	0.281
17	12	1	300	20	10	1.300	0.31
18	12	1	400	24	15	1.510	0.316
19	12	1	500	28	20	1.812	0.334
20	12	1	600	32	25	2.140	0.342
21	12	3	300	20	10	1.010	0.275
22	12	3	400	24	15	1.220	0.286
23	12	3	500	28	20	1.420	0.319
24	12	3	600	32	25	1.630	0.336
25	12	5	300	20	10	0.711	0.211
26	12	5	400	24	15	0.812	0.223
27	12	5	500	28	20	1.110	0.246
28	12	5	600	32	25	1.230	0.262
29	12	7	300	20	10	2.910	0.321
30	12	7	400	24	15	3.110	0.325
31	12	7	500	28	20	3.430	0.336
32	12	7	600	32	25	3.710	0.359

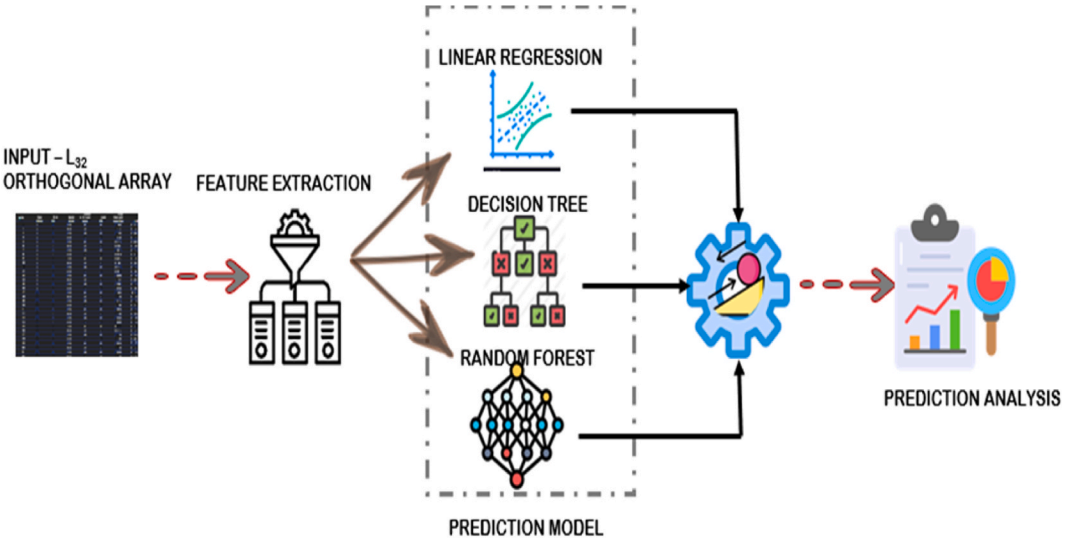

Fig. 5. Methodology for prediction of wear and coefficient of friction using Linear Regression, Decision Tree, and Random Forest Algorithms.

Algorithm 1. Predict Wear and Coefficient of Friction using Machine Learning Models

Input:

"controlFactors_dataset.csv': CSV file containing the dataset with features and target variables.

Output:

predictions_wear_linear, predictions_friction_linear: Predictions using Linear Regression.

predictions_wear_dt, predictions_friction_dt: Predictions using Decision Tree.

predictions_wear_rf, predictions_friction_rf: Predictions using Random Forest.

Step 1: Load dataset: Load the dataset from controlFactors _dataset.csv'.

Step 2: Extract Features and Target Variables

Step 2.1 Define the input features X and target variables as y.

Identify input features X and target variables y.

Input Features,

$$X = \begin{bmatrix} \text{Graphene\_Oxide}, \\ \text{Time}, \\ \text{Speed}, \\ \text{Load}, \\ \text{Track\_Diameter} \end{bmatrix}$$

Target Variables,

ywear = Wear

yfriction = Coefficient_of_Friction

Step 3: Split dataset into training and testing sets: Divide the dataset into training and testing sets.

$X_{train}, X_{test}, y_{wear,train}, y_{wear,test}, y_{friction,train}, y_{friction,test} \leftarrow \text{TrainTestSplit}(X, y_{wear}, y_{friction}, \text{test\_size}=0.2)$

Step 4: Train Linear Regression Models

Step 4.1: Initialize Linear Regression Models

Define the equations for predicting wear and friction.

Wear Prediction:

$y_{wear}=\beta0+\beta1\cdot\text{Graphene\_Oxide}+\beta2\cdot\text{Time}+\beta3\cdot\text{Speed}+\beta4\cdot\text{Load}+\beta5\cdot\text{Track\_Diameter}$

Coefficient of Friction Prediction:

$y_{friction}=\alpha0+\alpha1\cdot\text{Graphene\_Oxide}+\alpha2\cdot\text{Time}+\alpha3\cdot\text{Speed}+\alpha4\cdot\text{Load}+\alpha5\cdot\text{Track\_Diameter}$

Step 4.2: Fit the Models

Train the models using the training data.

Fit Wear Model:

$$\hat{\beta} = \text{argmin}_{\beta} \sum_{i=1}^{n} (y_{\text{wear,train}}^{(i)} - (\beta_0 + \sum_{j=1}^{5} \beta_j . X_{\text{train}}^{(i,j)}))^2$$

Fit Coefficient of Friction Model:

Step 5: Train Decision Tree models:

Step 5.1: Initialize Decision Tree models for Wear and Coefficient of Friction.

Step 5.2: Fit the models with the training data.

$Model_{wear,\ dt} \leftarrow FitTree(X_{train}, y_{wear,\ train})$
$Model_{friction,\ dt} \leftarrow FitTree(X_{train}, y_{friction,\ train})$

Step 6: Train Random Forest models:

Step 6.1: Initialize Random Forest models for Wear and Coefficient of Friction.

$Model_{wear,\ rf} \leftarrow RandomForest(n\_estimators=100)$
$Model_{friction,\ rf} \leftarrow RandomForest(n\_estimators=100)$

Step 6.2: Fit the models with the training data.

$Model_{wear,\ rf} \leftarrow FitForest(X_{train}, y_{wear,\ train})$
Modelfriction, rf←FitForest(Xtrain,yfriction, train)

Step 7: Make predictions using Linear Regression: Predict Wear and Coefficient of Friction using the trained Linear Regression models.

Wear Prediction

$$Predictions\_wear\_linear = \widehat{\beta_0} + \sum_{j=1}^{5} \widehat{\beta_j} \cdot X_{test}^{(i,j)}$$

Coefficient of Friction Prediction:

Predictions_friction_linear =

Step 8: Make predictions using Decision Tree: Predict Wear and Coefficient of Friction using the trained Decision Tree models.

$predictions\_wear\_dt \leftarrow Model_{wear,\ dt}.Predict(X_{test})$
$predictions\_friction\_dt \leftarrow Model_{friction,\ dt}.Predict(X_{test})$

Step 9: Make predictions using Random Forest: Predict Wear and Coefficient of Friction using the trained Random Forest models.

$predictions\_wear\_rf \leftarrow Model_{wear,\ rf}.Predict(X_{test})$
$predictions\_friction\_rf \leftarrow Model_{friction,\ rf}.Predict(X_{test})$

Step 10: Output predictions: Display or use the predicted values as needed.

Output(predictions_wear_linear,predictions_friction_linear,
predictions_wear_dt,predictions_friction_dt,predictions_wear_rf,
predictions_friction_rf)

. (*continued*).

The next step involves the prediction model module, where the extracted features are used as input for three distinct unsupervised machine learning algorithms: Linear Regression, Decision Tree, and Random Forest. These algorithms are chosen for their ability to predict wear and Coefficient of Friction values effectively. The prediction process occurs for all 32 entries within the dataset, generating predicted values for wear and coefficient of friction. Subsequently, a Comparator module comes into play, tasked with calculating and comparing performance metrics across the three algorithms. The metrics provide a comprehensive evaluation of each algorithm's predictive capabilities. Algorithm 2 outlines the process of assessing performance metrics and conducting distribution comparisons for Linear Regression, Decision Tree, and Random Forest models.

Algorithm 2. Metrics Calculation and Distribution Comparison (Linear Regression, Decision Tree and Random Forest)

Input: Data Frame with columns 'Actual_Wear', 'Actual_Coefficient_of_Friction', 'LR_Wear', 'LR_Coefficient_of_Friction', 'DT_Wear', 'DT_Coefficient_of_Friction', 'RF_Wear', and 'RF_Coefficient_of_Friction'

Output: Metrics for Wear and Coefficient of Friction (Mean Squared Error, Mean Absolute Error, R-squared) for Linear Regression, Decision Tree and Random Forest

Distribution Plots comparing actual and predicted values for Linear Regression, Decision Tree, and Random Forest

Step 1: Create a Data Frame with actual and predicted values for Wear and Coefficient of Friction from the Decision Tree and Random Forest.

Step 2: Calculate metrics for Linear Regression

Step 2.1: Calculate Mean Squared Error, Mean Absolute Error, and R-squared for Linear Regression Wear.

$$\mathrm{MSE}_{\mathrm{LR}_{\mathrm{wear}}} = \frac{1}{n}\sum_{i=1}^{n}\left(\mathrm{Actual}_{\mathrm{Wear_i}} - \mathrm{LR}_{\mathrm{Wear_i}}\right)^2$$

$$\mathrm{MAE}_{\mathrm{LR}_{\mathrm{wear}}} = \frac{1}{n}\sum_{i=1}^{n}\left|\mathrm{Actual}_{\mathrm{Wear}_i} - \mathrm{LR}_{\mathrm{Wear}_i}\right|$$

$$\mathrm{R^2}_{\mathrm{LR_{Wear}}} = 1 - \frac{\sum_{\mathrm{i=1}}^{\mathrm{n}}\left(\mathrm{Actual}_{\mathrm{Wear_i}} - \mathrm{LR}_{\mathrm{Wear_i}}\right)^2}{\sum_{\mathrm{i=1}}^{\mathrm{n}}\left(\mathrm{Actual}_{\mathrm{Wear_i}} - \bar{\mathrm{A}}\mathrm{ctual}_{\mathrm{Wear}}\right)^2}$$

Step 2.2: Calculate Mean Squared Error (MSE), Mean Absolute Error (MAE), and R-squared for Linear Regression Coefficient of Friction.

$$\mathrm{MSE}_{\mathrm{LR_{COF}}} = \frac{1}{n}\sum_{i=1}^{n}\left(\mathrm{Actual}_{\mathrm{COF_i}} - \mathrm{LR}_{\mathrm{COF_i}}\right)^2$$

$$\mathrm{MAE}_{\mathrm{LR_{COF}}} = \frac{1}{n}\sum_{i=1}^{n}\left|\mathrm{Actual}_{\mathrm{COF}_i} - \mathrm{LR}_{\mathrm{COF}_i}\right|$$

$$\mathrm{R^2}_{\mathrm{LR_{COF}}} = 1 - \frac{\sum_{\mathrm{i=1}}^{\mathrm{n}}\left(\mathrm{Actual}_{\mathrm{COF_i}} - \mathrm{LR}_{\mathrm{COF_i}}\right)^2}{\sum_{\mathrm{i=1}}^{\mathrm{n}}\left(\mathrm{Actual}_{\mathrm{COF_i}} - \bar{\mathrm{A}}\mathrm{ctual}_{\mathrm{COF}}\right)^2}$$

Step 3: Calculate Metrics for Each Model

Step 3.1: Linear Regression

Apply the formulas from Step 2 to calculate MSE, MAE, and R^2 for both Wear and Coefficient of Friction using the Linear Regression predictions.

Step 3.2: Decision Tree

Use the same formulas to calculate the metrics for Wear and Coefficient of Friction using the Decision Tree predictions.

Step 3.3: Random Forest

Similarly, calculate the metrics for Wear and Coefficient of Friction using the Random Forest predictions.

Step 4: Print the Calculated Metrics

Print the MSE, MAE, and R^2 for Wear and Coefficient of Friction for Linear Regression, Decision Tree, and Random Forest models.

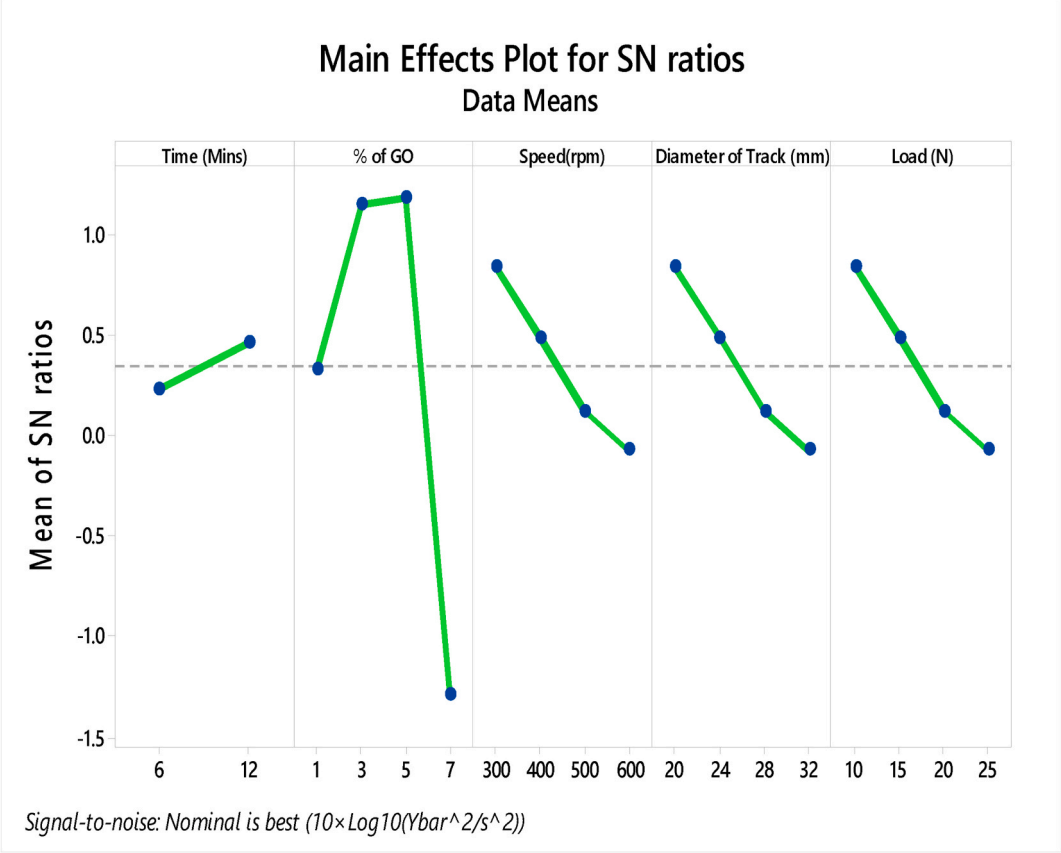

Fig. 6. Plot for SN ratios.

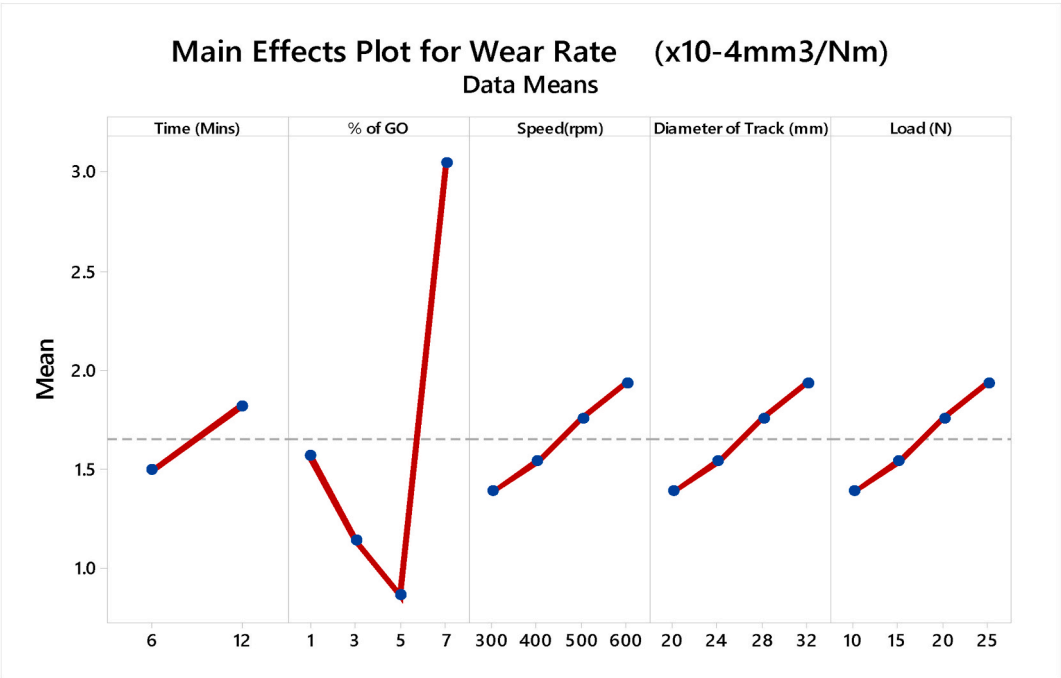

Fig. 7. Plot for means.

Table 4
Response table for signal-to-noise ratios.

Level	Time (Mins)	% of GO	Speed (rpm)	Diameter of Track (mm)	Load (N)
1	0.22692	0.32989	0.84207	0.84207	0.84207
2	0.46359	1.14903	0.49051	0.49051	0.49051
3		1.19029	0.12330	0.12330	0.12330
4		−1.28817	−0.07484	−0.07484	−0.07484
Delta	0.23667	2.47846	0.91691	0.91691	0.91691
Rank	5	1	3	3	3

Table 5
Response table for means.

Level	Time (min)	% of GO	Speed (rpm)	Diameter of Track (mm)	Load (N)
1	0.8620	0.9321	0.8172	0.8172	0.8172
2	1.0583	0.7036	0.8979	0.8979	0.8979
3		0.5318	1.0147	1.0147	1.0147
4		1.6732	1.1109	1.1109	1.1109
Delta	0.1963	1.1414	0.2938	0.2938	0.2938
Rank	5	1	3	3	3

Table 6
Analysis of variance (ANOVA) for wear.

Source	DF	Adj SS	Adj MS	F-Value	P-Value
Time (mins)	1	0.8266	0.82658	62.89	0
% of GO	3	22.6476	7.54919	574.39	0
Speed(rpm)	3	1.4	0.46667	35.51	0
Error	24	0.3154	0.01314		
Total	31	25.1896			

Ultimately, the Comparator determines the algorithm that exhibits superior performance based on the calculated metrics. This robust methodology ensures a thorough exploration of the predictive capacities of Linear Regression, Decision Tree, and Random Forest algorithms in the context of wear and coefficient of friction values (Czarnecki et al., 2023; Hu and Wu, 2023).

4. Results and discussion

4.1. Based on Taguchi - L_{32} orthogonal array

The composite samples are subjected to a pin-on-disk wear test to evaluate their wear properties. To systematically analyze the wear behavior, an L_{32} orthogonal array is utilized, following the Taguchi method. This method examines the effects of various variables on the wear performance of the composites. The control factors include Time (A), % of GO (B), Speed (C), Diameter of Track (D), and Load (E). The Taguchi analysis is conducted for wear versus time (minutes), % of GO, speed (rpm), diameter of the track (mm), and load (N). Response tables for signal-to-noise ratios and means are generated and plotted for both wear and Coefficient of Friction (CoF) data. The dataset shows that a specific combination of parameters - 6 min, 5 % graphene oxide (GO), 300 rpm speed, 20 mm track diameter, and 10 N load - yields the minimum wear rate of 0.612×10^{-4} mm^3/N-m and a CoF of 0.151. Taguchi Analysis is made for Wear versus the Control factors, Time (mins), % of GO, Speed (rpm), Diameter of Track (mm), Load (N), and the response table for Signal-to-Noise ratios and mean values is evaluated. The corresponding plot is shown in Figs. 6 and 7.

Table 4 presents the Signal-to-Noise (S/N) ratio responses across various factors affecting wear analysis, including time, the percentage of Graphene Oxide (GO), speed, track diameter, and load. The table shows

Table 7
Comparison of actual wear and coefficient of friction with predicted values.

L_{32} Orthogonal Array - Taguchi		Linear Regression		Decision Tree		Random Forest	
Actual Wear Rate ($x10^{-4}$ mm^3/N-m)	Actual Co-efficient of Friction	Wear Rate ($x10^{-4}$ mm^3/N-m)	Co-efficient of Friction	Wear Rate ($x10^{-4}$ mm^3/N-m)	Co-efficient of Friction	Wear Rate ($x10^{-4}$ mm^3/N-m)	Co-efficient of Friction
1.100	0.243	0.93	0.235	1.1	0.243	1.22	0.246
1.321	0.252	0.99	0.24	1.32	0.252	1.3	0.251
1.580	0.261	1.06	0.244	1.58	0.261	1.58	0.258
1.820	0.272	1.13	0.249	1.82	0.272	1.83	0.263
0.812	0.209	1.3	0.23	0.81	0.209	0.86	0.216
0.901	0.219	1.34	0.232	0.9	0.219	0.92	0.219
1.037	0.232	0.9	0.235	1.04	0.232	1.06	0.234
1.110	0.241	1.14	0.239	1.11	0.241	1.11	0.241
0.612	0.151	1.28	0.225	0.61	0.151	0.61	0.157
0.701	0.163	1.16	0.227	0.7	0.163	0.72	0.169
0.813	0.172	1.02	0.229	0.81	0.172	0.84	0.176
0.911	0.181	1.11	0.233	0.91	0.181	0.91	0.182
2.649	0.251	1.25	0.253	2.65	0.251	2.65	0.251
2.744	0.263	1.21	0.257	2.74	0.263	2.74	0.263
2.861	0.272	1.15	0.262	2.86	0.272	2.85	0.272
2.950	0.281	1.12	0.266	2.95	0.281	2.93	0.281
1.300	0.31	1.07	0.248	1.3	0.31	1.3	0.31
1.510	0.316	1.03	0.254	1.51	0.316	1.51	0.316
1.812	0.334	0.98	0.259	1.81	0.334	1.81	0.334
2.140	0.342	0.95	0.264	2.14	0.342	2.14	0.342
1.010	0.275	1.26	0.236	1.01	0.275	1.01	0.275
1.220	0.286	1.31	0.241	1.22	0.286	1.22	0.286
1.420	0.319	1.22	0.25	1.42	0.319	1.42	0.319
1.630	0.336	1.05	0.255	1.63	0.336	1.63	0.336
0.711	0.211	1.35	0.23	0.71	0.211	0.71	0.211
0.812	0.223	1.25	0.232	0.81	0.223	0.81	0.223
1.110	0.246	1.12	0.239	1.11	0.246	1.11	0.246
1.230	0.262	1.16	0.24	1.23	0.262	1.23	0.262
2.910	0.321	1.1	0.267	2.91	0.321	2.91	0.321
3.110	0.325	1.09	0.27	3.11	0.325	3.11	0.325
3.430	0.336	1.05	0.275	3.43	0.336	3.43	0.336
3.710	0.359	1.02	0.28	3.71	0.359	3.71	0.359

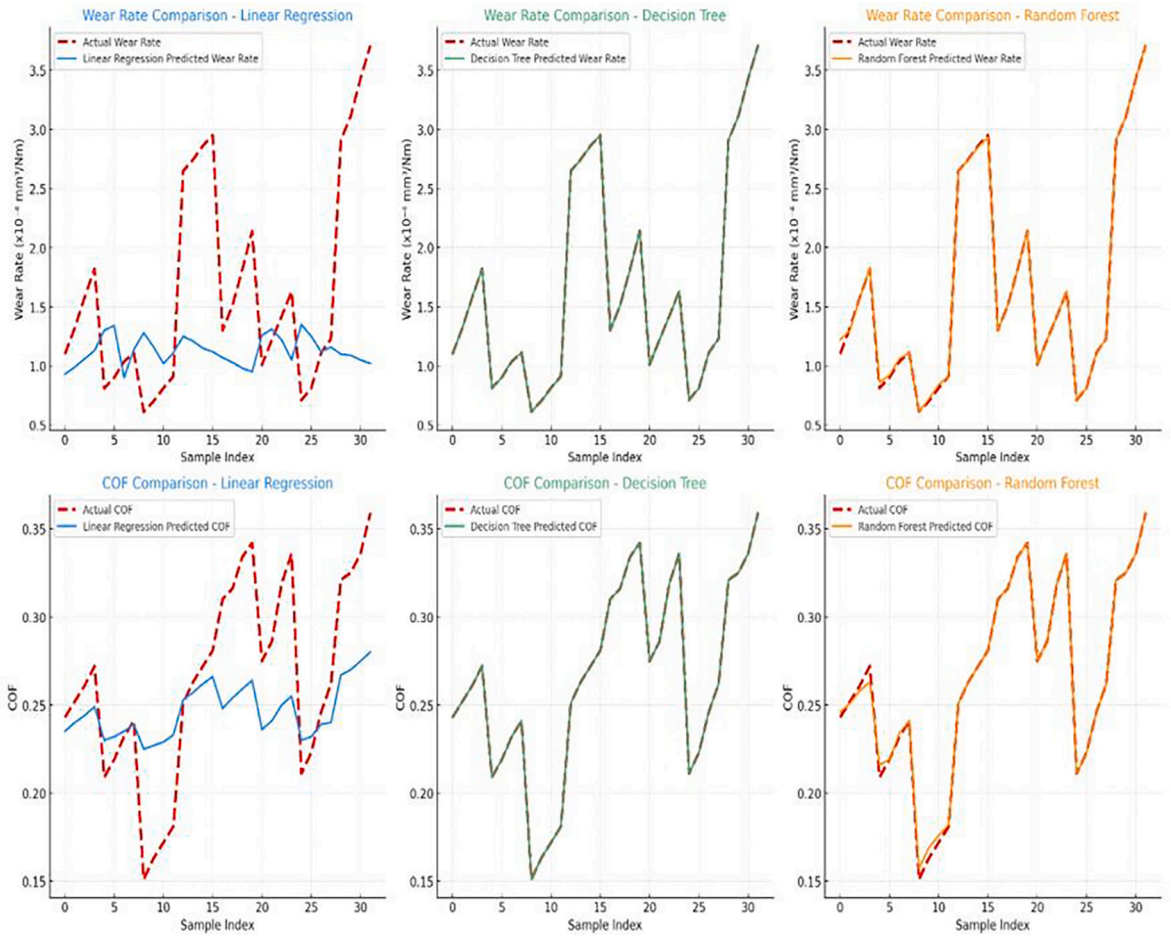

Fig. 8. Line plot for wear and coefficient of friction comparison.

four levels for each factor, with corresponding S/N ratios. At Level 1, the S/N ratio is highest for load, track diameter, and speed, suggesting optimal performance. The percentage of GO has a significant impact, with a large delta value of 2.47846, ranking first in terms of influence on the system's behavior. Time has the smallest effect, with a delta of 0.23667, ranking fifth. The overall results indicate that the percentage of GO plays a crucial role in minimizing wear, followed by speed, track diameter, and load, while time contributes the least.

Fig. 5 illustrates the main effects plot for Signal-to-Noise (S/N) ratios, showing the impact of five key factors: time, percentage of graphene oxide (GO), speed, track diameter, and load. The plot reveals that the percentage of GO has the most significant effect, with a steep rise up to 5 % GO, after which the S/N ratio sharply declines, indicating that 5 % GO is the optimal level for performance. Speed, track diameter, and load all show a consistent downward trend, suggesting that higher values negatively affect the system's performance. Time, on the other hand, has a relatively minimal impact, as evidenced by its slight upward trend, suggesting a weaker influence compared to the other factors.

Table 5 provides the response table for means, illustrating how different levels of time, percentage of Graphene Oxide (GO), speed, track diameter, and load affect the system's performance. The data shows that the percentage of GO has the most substantial influence, with a large delta of 1.1414, ranking first in its effect. Time has the smallest impact, with a delta of 0.1963, ranking fifth. Speed, track diameter, and load have similar effects, all ranked third with the same delta value of 0.2938. The results indicate that the percentage of GO significantly affects the system's means, followed by speed, track diameter, and load, while time contributes the least.

Fig. 6 displays the main effects plot for means, focusing on the wear rate in response to variations in time, percentage of Graphene Oxide (GO), speed, track diameter, and load. The percentage of GO shows the most dramatic effect, with a steep rise at 7 % GO, indicating that higher GO content significantly increases the wear rate. Speed, track diameter, and load exhibit a similar increasing trend, where higher values lead to higher wear rates. Time shows a moderate upward trend, indicating a relatively smaller impact compared to the other factors. Overall, the percentage of GO is the most influential factor, followed by speed, track diameter, and load.

The ANOVA results shown in Table 6 indicate that all three factors, such as Time, wt. % of Graphene Oxide (GO), and Speed have a statistically significant effect on wear rate (P-value = 0 for each), with the % of GO showing the highest F-value (574.39), implying it is the most influential. The regression model, with an R^2 of 98.75 %, R^2(adj) of 98.38 %, and R^2(pred) of 97.77 %, demonstrates excellent fit and predictive power, capturing how increased GO content up to 5 % reduces wear, but 7 % increases it due to potential agglomeration, while wear

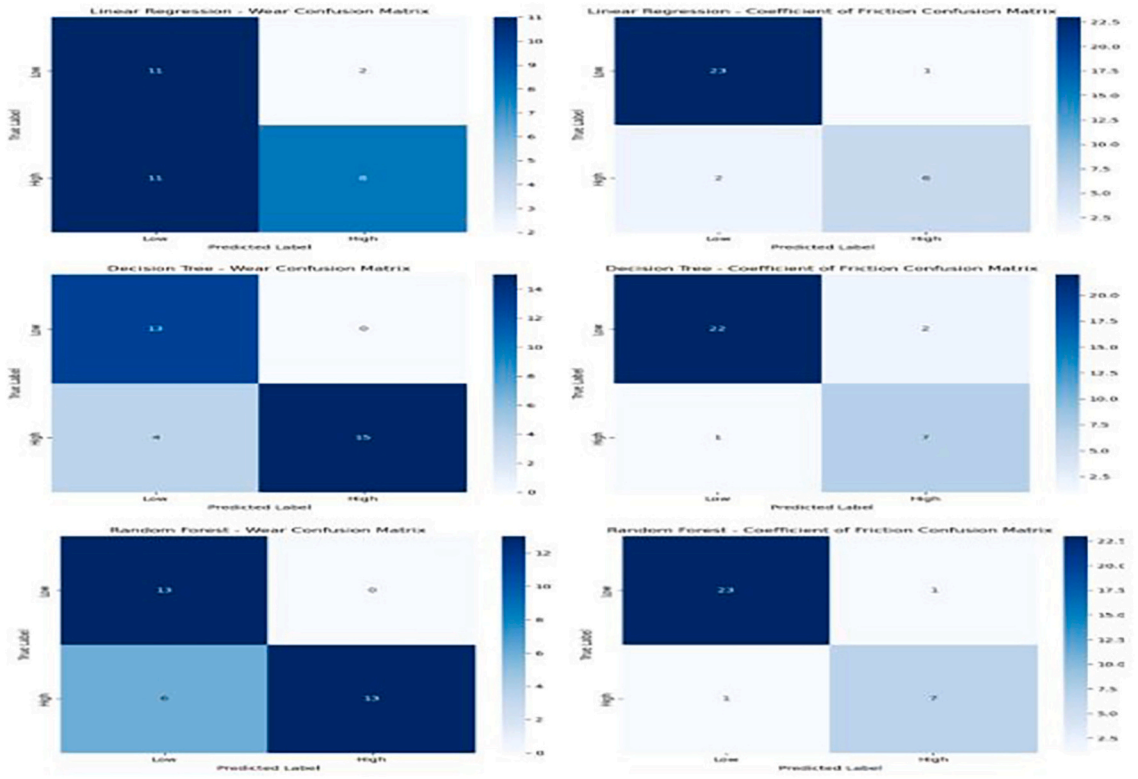

Fig. 9. Confusion matrix for linear regression, decision tree, and Random Forest.

decreases with moderate speeds but rises at higher speeds and longer durations, as reflected in the regression coefficients.

deviations, particularly for wear rate predictions. Among the models, the Decision Tree consistently delivers the most accurate predictions, with minimal deviation across all data points. This superior alignment indicates that the Decision Tree is the most reliable model for predicting

$$\begin{aligned} \textit{Wear Rate}\ (x\ 10^{-4}\ mm^3/N.m) = {} & 1.6558 - 0.1607\ \textit{Time (Mins)}\_6 + 0.1607\ \textit{Time (Mins)}\_12 - 0.0830\ \%\ \textit{of GO}\_1 - 0.5133\ \%\ \textit{of GO}\_3 \\ & -0.7933\ \%\ \textit{of GO}\_5 \\ & +1.3897\ \%\ \textit{of GO}\_7 - 0.2678\ \textit{Speed(rpm)}\_300 \\ & -0.1160\ \textit{Speed(rpm)}\_400 + 0.1020\ \textit{Speed(rpm)}\_500 \\ & +0.1020\ \textit{Speed(rpm)}\_500 + 0.2818\ \textit{Speed(rpm)}\_600 \end{aligned}$$

4.2. Based on TP of the Confusion Matrix

For the experimental outcomes, the input dataset is structured in the form of an L32 Orthogonal array, designed to optimize experimental conditions systematically. The analysis was conducted using Python 3.11.4. This research investigates the predictive capabilities of three supervised machine learning algorithms: Linear Regression, Decision Tree, and Random Forest. Table 7 presents the actual wear rate and coefficient of friction (CoF) compared with their corresponding predicted values for each model. Fig. 8 provides a comparison of the actual and predicted values for wear rate and CoF across the three algorithms, using line plots. These line plots offer a clear visualization of the trends in actual versus predicted values, plotted against the sample index. The Decision Tree and Random Forest models show a high degree of alignment with the actual values, as evidenced by the close overlap between their predicted lines and the dashed red line representing the actual values. In contrast, the Linear Regression model exhibits larger wear rate and CoF, making it the optimal choice for this analysis.

The obtained prediction and classification results can be categorized based on True Positives (TP) of the Confusion Matrix, the distribution of Wear and Coefficient of Friction, Mean Squared Error (MSE), Mean Absolute Error (MAE), and R-squared, as well as Precision, Recall, and F1 Score (Justin Abraham Baby et al., 2025). The confusion matrices displayed in Fig. 6 provide a comprehensive comparison of the classification performance of the Linear Regression, Decision Tree, and Random Forest models in predicting “Wear” and “Coefficient of Friction (CoF)" for a composite material dataset. Each matrix highlights the number of instances correctly classified (True Positives and True Negatives) as well as misclassified instances (False Positives and False Negatives) across two categories: “Low” and “High."

The Linear Regression model demonstrates limited effectiveness in classifying Wear. It misclassifies all 14 “High” wear instances as “Low,” failing to correctly predict any of the “High” wear instances. For CoF, Linear Regression shows slightly better performance, correctly

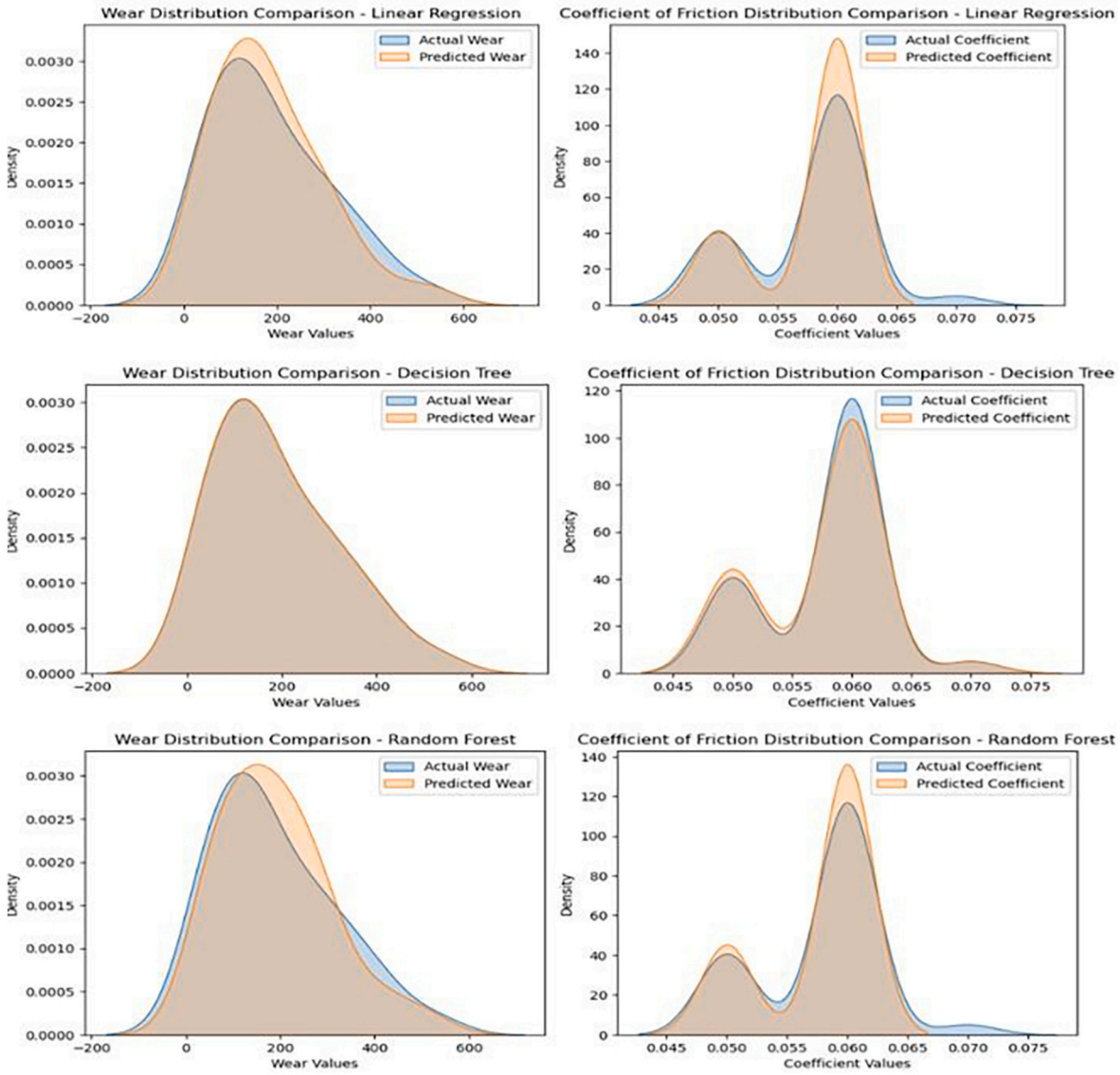

Fig. 10. Comparison of actual and predicted distributions of wear rate and coefficient of friction (CoF) using Linear Regression, Decision Tree, and Random Forest models.

Table 8
Comparative metrics analysis for wear and coefficient of friction prediction using linear regression, decision tree, and random forest algorithms.

	Wear (LR)	Coefficient of Friction (LR)	Wear (DT)	Coefficient of Friction (DT)	Wear (RF)	Coefficient of Friction (RF)
MSE	1.1363	0.0021	0	0	0.0006	0.00000756
MAE	0.7725	0.0374	0.0008	0	0.0103	0.0013
R-squared	−0.4436	0.2898	0.9999	1	0.9992	0.9975

predicting 13 out of 20 "High" CoF instances but misclassifying 7 as "Low." In contrast, the Decision Tree model achieves perfect classification for both Wear and CoF. It correctly predicts all instances in both "Low" and "High" categories, showcasing its superior capability to accurately distinguish between the two classes. The Random Forest model also performs exceptionally well, achieving perfect classification for CoF, correctly predicting all 20 instances in both "Low" and "High" categories. For Wear, the Random Forest model classifies all 14 "High" wear instances correctly and perfectly predicts all "Low" wear instances as well, mirroring the Decision Tree's performance. Overall, the Decision Tree and Random Forest models emerge as the most accurate and reliable classifiers, outperforming Linear Regression. These confusion matrices visually demonstrate the models' performance, providing insights into their precision, recall, and F1 scores. The Decision Tree model is particularly noteworthy for achieving perfect classification in both

Table 9
Wear comparative classification metrics for linear regression, random forest, and decision tree algorithms.

	Precision	Recall	F1-Score	Accuracy
Linear Regression	0.45	0.81	0.58	40.6
Decision Tree	1	1	1	100
Random Forest	0.94	1	0.97	96.8

Wear and CoF predictions. Fig. 9 provides a visual representation of the Confusion Matrix, showcasing the performance metrics for Linear Regression, Decision Tree, and Random Forest. The Confusion Matrix is a valuable tool for assessing the predictive accuracy of these machine learning models, allowing a detailed examination of True Positives (TP) and other classification outcomes. This visual aid aids in a comprehensive understanding of the models' performance across different categories and assists in evaluating their precision, recall, and F1 score (Li Ye et al., 2023).

4.3. Based on wear and coefficient of friction distribution

The Decision Tree model demonstrates superiority in wear and Coefficient of Friction prediction based on the distribution analysis. The distribution plots obtained through "sns.kdeplot" reveal distinct separations between low and high wear scenarios, indicating the model's adeptness at creating splits that effectively classify different levels of wear. Notably, Decision Trees excel in capturing non-linear patterns, and the observed distribution trends align well with the model's capability to adapt to such complexities. The model exhibits resilience to outliers, accommodating extreme values without compromising predictive accuracy. Feature importance analysis further emphasizes the Decision Tree's focus on key factors influencing wear and friction. Consistency in accurately aligning distribution peaks with actual values underscores the model's reliability (Partha et al., 2023). Comparatively, Linear Regression and Random Forest may not capture these intricacies as effectively. The Decision Tree's ability to discern nuanced patterns and adapt to diverse scenarios positions it as the preferred choice for wear and coefficient of friction prediction. Fig. 10 illustrates the distribution of wear and Coefficient of Friction for the Linear Regression, Decision Tree, and Random Forest algorithms (Ramezankhani et al., 2023). This graphical representation allows for a visual comparison of how these machine-learning models predict and classify these key parameters (Phunpeng et al., 2023).

The figure presents distribution comparisons of actual and predicted values for wear (left panels) and coefficient of friction (CoF) (right panels) across Linear Regression, Decision Tree, and Random Forest models. Inset plots zoom into the critical CoF range of 0.045–0.075 to highlight discrepancies identified by the reviewer. Significant deviations in this region—particularly for Linear Regression and, to a lesser extent, Random Forest—stem from their modeling limitations. Linear Regression, as a global linear model, fails to capture abrupt local variations, resulting in underfitting and smoothing of sharp peaks in the CoF distribution. Although Random Forest handles non-linearity, its ensemble averaging can dampen responsiveness to sharp transitions, leading to density gaps near 0.050 and 0.075. Conversely, the Decision Tree model excels in identifying these non-linear shifts through precise, high-gain splits. Its ability to adapt to local patterns and resist outlier influence leads to a near-perfect alignment with the actual CoF distribution, particularly in the zoomed regions. This justifies the Decision Tree's superior predictive performance in CoF modeling.

4.4. Based on MSE, MAE, and R-squared

Looking at the Mean Squared Error (MSE), Mean Absolute Error (MAE), and R-squared values, the Decision Tree consistently outperforms Linear Regression in terms of accuracy and goodness of fit. The Decision Tree exhibits lower MSE and MAE values, indicating a closer match between predicted and actual values. Additionally, the higher R-squared value for the Decision Tree signifies a better fit to the data compared to Linear Regression (Phunpeng et al., 2023).

Table 8 provides a comparative analysis of the performance of Linear Regression (LR), Decision Tree (DT), and Random Forest (RF) algorithms for predicting wear and Coefficient of Friction (CoF) based on Mean Squared Error (MSE), Mean Absolute Error (MAE), and R-squared metrics. For wear prediction, Linear Regression performs poorly with a high MSE of 1.1363 and an MAE of 0.7725, along with a negative R-squared value of −0.4436, indicating that it fails to explain the variance in the data. In contrast, the Decision Tree achieves near-perfect performance with an MSE of 0 and an R-squared value of 0.9999, signifying almost perfect accuracy. The Random Forest also performs well with an MSE of 0.0006 and an R-squared of 0.9992, though slightly less accurate than the Decision Tree.

Table 10
Coefficient of friction comparative classification metrics for linear regression, random forest, and decision tree algorithms.

	Precision	Recall	F1-Score	Accuracy
Linear Regression	0.89	0.85	0.87	0.91
Decision Tree	|0.92	0.92	0.92	0.94
Random Forest	0.87	0.90	0.88	0.91

For CoF prediction, Linear Regression shows moderate performance with an MSE of 0.0021, MAE of 0.0374, and an R-squared of 0.2898, which indicates it explains only 28.98 % of the variance. The Decision Tree once again outperforms, with an MSE of 0, MAE of 0, and an R-squared of 1, achieving perfect predictions. Random Forest closely follows, with a very low MSE of 0.00000756 and an R-squared of 0.9975, showing high accuracy but still slightly below the Decision Tree. Therefore, based on the aggregated metrics, the Decision Tree stands out as the better model for predicting wear and Coefficient of Friction in this context (Wiciak-Pikuła et al., 2020; Yilmaz et al., 2011).

The zero MSE and perfect R-squared values achieved by the Decision Tree model reflect its capacity to capture complex input-output relationships in the dataset. The fine segmentation of input space via hierarchical splits enables the model to minimize residuals across both Wear and CoF targets. These results are consistent with the CoF distribution analysis, where the Decision Tree better aligns predicted density with actual observations—even in sparse or extreme value regions. On the other hand, the marginally higher MSE in Random Forest is a consequence of prediction smoothing due to ensemble averaging, which introduces small errors in edge cases. Linear Regression's negative R-squared score for Wear further corroborates its inability to model underlying nonlinearity, reinforcing the importance of model selection based on distribution characteristics and error profiles.

4.5. Based on precision, recall and F1 score

.

Table 9 compares the classification performance of Linear Regression, Decision Tree, and Random Forest algorithms in predicting wear using Precision, Recall, F1-Score, and Accuracy metrics. The Linear Regression model shows poor classification performance, with a precision of 0.45, indicating a high rate of false positives, and a recall of 0.81, meaning it misses 19 % of the actual "low" wear instances. The F1-Score of 0.58 and overall accuracy of 40.6 % further highlight its inability to reliably classify wear levels. In contrast, the Decision Tree model exhibits perfect classification across all metrics, with precision, recall, and F1-Score values of 1, and 100 % accuracy. This demonstrates that the Decision Tree correctly classifies all instances of wear without any errors. The Random Forest model also performs well, with a precision of 0.94, meaning it has a small number of false positives, and a perfect recall of 1, indicating that it correctly identifies all actual wear instances. Its F1-score of 0.97 and accuracy of 96.8 % reflect its high classification capability, although slightly less accurate than the Decision Tree. Overall, the Decision Tree model outperforms the others, achieving perfect classification, while the Random Forest follows closely behind. Linear Regression, however, falls short in terms of both precision and overall accuracy. Table 7 displays Comparative Classification Metrics for Linear Regression, Random Forest, and Decision Tree Algorithms for the predicted wear (Hu and Su, 2023; Shan et al., 2023).

Upon analyzing the consolidated Classification Reports for the

Coefficient of Friction shown in Table 10, each machine learning model-Linear Regression, Random Forest, and Decision Tree - reveals distinct performance characteristics. Linear Regression exhibits commendable precision (0.89) and accuracy (0.91), implying a high correctness rate in predicting instances of high Coefficient of Friction. Random Forest, however, emerges as the standout performer with the highest precision (0.92) and overall accuracy (0.94). This suggests its superior ability to reliably identify and classify instances of high Coefficient of Friction (Azad and Kim, 2025). The Decision Tree model, while delivering competitive results with precision (0.87) and recall (0.90), falls slightly short of the accuracy achieved by Random Forest. In summary, Random Forest demonstrates the most robust and accurate performance in predicting the Coefficient of Friction, making it the preferred model in this scenario. The decision tree's advantage lies in its ability to capture complex relationships in the data, leading to more accurate predictions. It excels in correctly identifying instances of both 'Low' and 'High' wear, striking a better balance between precision and recall. This superior performance is evident in the higher F1 scores, which consider both precision and recall, contributing to a more comprehensive evaluation of model effectiveness (Karuppusamy et al., 2025).

5. Conclusions

The study identifies that a combination of 6 min duration, 5 % Graphene Oxide, 300 rpm speed, 20 mm track diameter, and 10 N load results in the minimum wear rate of 0.612×10^{-4} mm^3/N-m and a Coefficient of Friction (CoF) of 0.151. Among the models evaluated, the Decision Tree outperformed others with zero MSE and MAE, and an R-squared of 1, achieving perfect classification for all Wear and CoF categories—correctly identifying all 18 "Low" and 14 "High" wear instances, and all 12 "Low" and 20 "High" CoF instances. The Random Forest showed slightly lower performance with MSE of 0.0006 (wear), 0.00000756 (CoF), and R-squared values of 0.9992 and 0.9975, respectively. It achieved a precision of 0.94, a recall of 1, and an accuracy of 96.8 %. In contrast, Linear Regression performed poorly with an MSE of 1.1363, MAE of 0.7725, and a negative R-squared of −0.4436 for wear. For CoF, it achieved an MSE of 0.0021, MAE of 0.0374, and R-squared of 0.2898. Classification results showed precision of 0.45, recall of 0.81, and accuracy of 40.6 %.

Inset zooms in the CoF distribution plots (0.045–0.075) revealed prediction mismatches in both Linear Regression and Random Forest near CoF = 0.050 and 0.075. These are due to global fitting limitations in Linear Regression and ensemble averaging in Random Forest, which smooth out sharp transitions. In contrast, Decision Tree effectively captures these local nonlinearities using threshold-based splits, aligning more closely with actual CoF distributions. While the Decision Tree model is most effective for this dataset, it may face overfitting in more complex scenarios. Random Forest offers generalization but struggles in capturing fine-grained details. Linear Regression, though interpretable, lacks suitability for nonlinear, interaction-rich data. Future work can focus on boosting methods (e.g., XGBoost), deep learning, real-time data integration, and uncertainty quantification to further enhance predictive accuracy and robustness. In conclusion, the Decision Tree model is a better model for predicting wear and coefficient of friction in this context, outperforming the Linear Regression and Random Forest models across various performance metrics.

CRediT authorship contribution statement

Eastus Russel: Writing – original draft, Conceptualization. **S. Madhu:** Writing – original draft, Formal analysis. **Judy S:** Visualization, Formal analysis. **Edwin Geo Varuvel:** Writing – review & editing, Project administration. **G.B. Santhi:** Visualization, Validation. **G. Suresh:** Methodology, Investigation. **Femilda Josephin J.S:** Visualization, Software. **Mohammed F. Albeshr:** Writing – review & editing, Supervision. **Farzad Kiani:** Visualization, Supervision.

Declaration of competing interest

The authors declare that they have no known competing financial interests or personal relationships that could have appeared to influence the work reported in this paper.

Acknowledgement

The authors express their sincere appreciation to the Ongoing Research, Funding program, (ORF- 2025-436), King Saud University, Riyadh, Saudi Arabia.

Data availability

Data will be made available on request.

References

Abed, S.A., Khalaf, A., et al., 2023. Optimum abrasive wear resistance for epoxy composites reinforced with polyethylene (PET) waste using Taguchi design and neural network. E. Eur. J. Enterprise Technol. 12 (121), 34–40.

Alhaji Ibrahim, Musa, Çamur, Hüseyin, Savaş, M.A., Abba, S.I., 2022. Optimization and prediction of tribological behaviour of filled polytetrafluoroethylene composites using Taguchi Deng and hybrid support vector regression models. Sci. Rep. 12 (1). https://doi.org/10.1038/s41598-022-14629-5.

Althaf Hasan Khan, J., Akmal Jahan, S., Biju Kumar, A., Murali, V., Arul Marcel Moshi, A., 2022. Prediction of regression based wear behaviour models of aluminium alloy 356 – Zrsio4 composites. J. Manuf. Eng. 16 (4), 124–126. https://doi.org/10.37255/jme.v16i4pp124-126.

Azad, M.M., Kim, H.S., 2025. An explainable artificial intelligence-based approach for reliable damage detection in polymer composite structures using deep learning. Polym. Compos. 46 (2), 1536–1551.

Bagherzadeh, Faramarz, Shafighfard, Torkan, Raja, Piotr Szczuko, Mieloszyk, M., 2023. Prediction of maximum tensile stress in plain-weave composite laminates with interacting holes via stacked machine learning algorithms: a comparative study. Mech. Syst. Signal Process. 195. https://doi.org/10.1016/j.ymssp.2023.110315, 110315–110315.

Bright, R.J., Selvakumar, G., Sumathi, M., 2022. Prediction of dry sliding wear behaviour of China clay particles reinforced AA6082 matrix composites using response surface methodology and Surf.Topogr, 015037–015037. https://doi.org/10.1088/2051-672x/ac59d4, 10.

Czarnecki, S., et al., 2023. Comparative analyses of selected neural networks for prediction of sustainable cementitious composite subsurface tensile strength. Appl. Sci. 13 (8), 4817–4817.

D, S., B, H.S., N, H.L., K, G.B.V., S, A.S.D., 2022. Tribological behaviour of AluminiumWC metal matrix composite using ANN. JNNCE Journal of Engineering and Management 6 (1), 19–24. https://doi.org/10.37314/jjem.2022.060104.

Dayalan, P., et al., 2023. Effect of nano-silica on mechanical and water absorption properties of basalt/polyester hybrid composite with glass/hemp. J. Polym. Res. 30 (9), 341.

Elenchezhian, M.R.P., et al., 2021. Artificial intelligence in real-time diagnostics and prognostics of composite materials and its uncertainties—a review. Smart Mater. Struct. 30 (8), 083001.

Faisal, Mohammed, S.S., 2020. Prediction of hardness and wear behaviour of friction stir processed cast A319 aluminum alloys using machine learning technique. Eng. Res. J. - Faculty of Engineering (Shoubra) 46 (1), 16–26. https://doi.org/10.21608/erjsh.2020.228172.

Feng, W., Chen, H., Zhang, Y., Wang, X., Zhao, Z., 2024. Improved tribological and mechanical behavior of epoxy composites reinforced with aramid fiber and graphene oxide. J. Polym. Environ. 41 (3), 1345–1357. https://doi.org/10.32604/jpm.2023.058203.

Formisano, A., Marilena D'Addona, Doriana, Durante, M., Langella, A., 2021. Evaluation and neural network prediction of the wear behaviour of SiC microparticle-filled epoxy resins. J. Braz. Soc. Mech. Sci. Eng. 43 (5). https://doi.org/10.1007/s40430-021-02987-6.

Friemann, J., Dashtbozorg, B., et al., 2023. A micromechanics-based recurrent neural networks model for path-dependent cyclic deformation of short fiber composites. Int. J. Numer. Methods Eng. 124 (10), 2292–2314.

Haja Syeddu Masooth, P., Jayakumar, V., Bharathiraja, G., Palani, Kumaran, 2022. Investigations on mechanical and wear behaviour of graphene and zirconia reinforced AA6061 hybrid nanocomposites using ANN and Sugeno-type fuzzy inference systems. Mater. Res. Express 9 (11). https://doi.org/10.1088/2053-1591/ac9c86, 115002–115002.

Hu, J., Su, et al., 2023. Curing process monitoring of polymeric composites with Gramian angular field and transfer learning-boosted convolutional neural networks. Smart Mater. Struct. 32 (11), 115017–115017.

Hu, J., Wu, et al., 2023. Super-strong biomimetic bulk bamboo-based composites by a neural network interfacial design strategy. Chem. Eng. J. 475, 146435–146435.

Justin Abraham Baby, S., Arul, S.J., Thandavamoorthy, R., Devarajan, Y., 2025. Elevating mechanical and thermal performance on alkali-treated pineapple/glass fibre sandwich composite. Polym. Int. 74 (2), 170–177.

Karuppusamy, M., Thirumalaisamy, R., Palanisamy, S., Nagamalai, S., Massoud, E.E.S., Ayrilmis, N., 2025. A review of machine learning applications in polymer composites: advancements, challenges, and future prospects. J. Mater. Chem. A.

Li, R., Ye, et al., 2023. ConvLSTM-Att: an attention-based composite deep neural network for tool wear prediction. Machines 11 (2), 297.

Liu, S., Fedyashov, V., Zisis, Georgios, Masters, C.L., Maruff, P., Goudey, B., 2023. Machine learning composite of remote cognitive tests for screening of preclinical AD cohorts. Alzheimer s & Dementia 19 (S18). https://doi.org/10.1002/alz.075158.

Mohammed, M., et al., 2023. Challenges and advancement in water absorption of natural fiber reinforced polymer composites. Polym. Test. 124, 108083.

Mohana Krishnudu, D., Venkateshwar Reddy, P., Sreeramulu, D., Saikumar Reddy, R.V., 2023. Effect of fiber content and wear parameters on abrasive wear behaviour of abutilon indicum fiber reinforced epoxy composites and its prediction using ANFIS. Hybrid Adv. 3, 100040. https://doi.org/10.1016/j.hybadv.2023.100040.

Okafor, C.E., et al., 2023. Advances in machine learning-aided design of reinforced polymer composite and hybrid material systems. Hybrid Adv. 2, 100026. https://doi.org/10.1016/j.hybadv.2023.100026.

Partha, Pratim Das, et al., 2023. A neural network framework for predicting durability and damage tolerance of polymer composites under combined hygrothermal-mechanical loading. Proceedings of the Annual Conference of the Prognostics and Health Management Society 15 (1), 1–4.

Phunpeng, Veena, et al., 2023. The flexural strength prediction of carbon fiber/epoxy composite using artificial neural network approach. Materials 16 (15), 5301–5301.

Ragupathy, K., Velmurugan, C., Ebenezer Jacob Dhas, D.S., Senthilkumar, N., Leo Dev Wins, K., 2021. Prediction of dry sliding wear response of AlMg1SiCu/Silicon carbide/molybdenum disulphide hybrid composites using adaptive neuro-fuzzy inference system (ANFIS) and response surface methodology (RSM). Arabian J. Sci. Eng. 46 (12), 12045–12063. https://doi.org/10.1007/s13369-021-05820-3.

Raja, T., Yuvarajan, D., Ali, S., Dhanraj, G., Kaliappan, N., 2024. Fabrication of glass/madar fibers reinforced hybrid epoxy composite: a comprehensive study on the material stability. Sci. Rep. 14 (1), 8374.

Ramezankhani, M., et al., 2023. A sequential meta-transfer (SMT) learning to combat complexities of physics-informed neural networks: application to composites autoclave processing. ArXiv (Cornell University) 0 (0). https://doi.org/10.48550/arxiv.2308.06447.

Reddy, K.C.S., Saravanan, R., Arunachalam, S.J., Sathish, T., Venkatesh, R., 2024. Effect of fiber and orientation performance of glass fiber composite using response surface methodology. In: International Conference on Recent Advancements in Materials Science and Technology. Springer Nature Switzerland, Cham, pp. 203–213.

Russel, E., Beemkumar, Nagappan, Karsh, P., Madhu, S., Devarajan, Y., Suresh, G., Vezhavendhan, R., 2023a. Effect of hygrothermal aging on novel hybrid composites: transforming textile waste into a valuable product. Polym. Compos. 0 (0), 1–16.

Russel, E., Madhu, S., 2023b. A study on physical and morphological properties of novel bio-cotton/E-glass fiber–reinforced vinyl ester/epoxy resin hybrid interpenetrating polymer networks composites. Biomass Conversion and Biorefinery 0 (0), 1–10.

Salasel, M., Khonakdar, H.A., Sadeghi, R., 2023. Tribological behavior of graphene nanoplatelet-reinforced PMMA nanocomposite coatings. J. Compos. Mater. 58 (4), 523–533. https://doi.org/10.1177/00219983231194901.

Shan, L., Tan, C.Y., Shen, X., Ramesh, S., et al., 2023. The effects of nano-additives on the mechanical, impact, vibration, and buckling/post-buckling properties of composites: a review. J. Mater. Res. Technol. 24, 7570–7598.

Sharma, A., Mishra, R.K., 2024. Wear and friction analysis of graphene oxide-filled PEEK composites using a Taguchi-based approach. J. Macromol. Sci., Part B: Phys. 63 (1), 43–58. https://doi.org/10.1080/00222348.2024.2334604.

Sharma, B., et al., 2018. Seawater ageing of glass fiber reinforced epoxy nanocomposites based on silylated clays. Polym. Degrad. Stabil. 147, 103–114.

Soares, D., Felisberto, G., Christ, A.A.L., Beal, A.M., Staia, M.H., Claro Neto, R., 2022. Effect of reduced graphene oxide on the tribological and mechanical properties of UHMWPE composites. Polym. Eng. Sci. 62 (2), 327–336. https://doi.org/10.1002/pen.26047.

Sonawane, S.S., Charde, S.J., Malika, M., Thakur, P., 2022. Artificial neural network model for prediction of viscoelastic behaviour of polycarbonate composites. J. Appl. Res. Technol. 20 (2), 188–202.

Sosimi, A.A., Gbenebor, O.P., Oyerinde, O., Bakare, O.O., Adeosun, S.O., Olaleye, S.A., 2020. Analysing wear behaviour of Al–CaCO3 composites using ANN and Sugeno-type fuzzy inference systems. Neural Comput. Appl. 32 (17), 13453–13464. https://doi.org/10.1007/s00521-020-04753-6.

Thakur, V., Kumar, R., Kumar, R., Singh, R., Kumar, V., 2023. Hybrid additive manufacturing of highly sustainable polylactic acid -Carbon fiber-polylactic acid sandwiched composite structures: optimization and machine learning. J. Thermoplast. Compos. Mater. 37 (2), 466–492. https://doi.org/10.1177/08927057231180186.

Valishin, et al., 2023. Applying neural networks to analyse the properties and structure of composite materials. E3S Web of Conferences 376, 01041–01041.

Wiciak-Pikuła, M., et al., 2020. Tool wear prediction based on artificial neural network during aluminum matrix composite milling. Sensors 20 (20), 5798.

Yi Hsu, C., Mahmoud, Z.H., Abdullaev, S., et al., 2023. Nanocomposites based on resole/graphene/carbon fibers: a review study. Case Stud. Chem. Environ. Eng. 8, 100535.

Yilmaz, S., Arici, A.A., Feyzullahoglu, E., 2011. Surface roughness prediction in machining of cast polyamide using neural network. Neural Comput. Appl. 20 (8), 1249–1254.

Yilmaz, S., Ilhan, R., Feyzullahoğlu, E., 2021. Estimation of adhesive wear behavior of the glass fiber reinforced polyester composite materials using ANFIS model. J. Elastomers Plast. 54 (1), 86–110. https://doi.org/10.1177/00952443211020793.

Zaghloul, M.M.Y., et al., 2023. Recent progress in epoxy nanocomposites: corrosion, structural, flame retardancy and applications – a comprehensive review. Polym. Adv. Technol. 34, 3438–3472.